Applied Geochemistry 25 (2010) 593–601

Contents lists available at ScienceDirect

Applied Geochemistry

journal homepage: www.elsevier.com/locate/apgeochem

Nitrogen as the carrier gas for helium emission along an active fault in NW Taiwan

Wei-Li Hong [a], Tsanyao Frank Yang [a,*], Vivek Walia [b], Shih-Jung Lin [b], Ching-Chou Fu [a], Yue-Gau Chen [a], Yuji Sano [c], Cheng-Hong Chen [a], Kuo-Liang Wen [b,d]

[a] Department of Geosciences, National Taiwan University, No. 1, Sec. 4, Roosevelt Road, Taipei 10699, Taiwan
[b] National Center for Research on Earthquake Engineering, National Applied Research Laboratories, Taipei 106, Taiwan
[c] Center for Advanced Marine Research, Ocean Research Institute, The University of Tokyo, Tokyo 164-8639, Japan
[d] Department of Earth Sciences and Institute of Geophysics, National Central University, Jhong-li 32054, Taiwan

ARTICLE INFO

Article history:
Available online 25 January 2010

ABSTRACT

Variations of He gas concentration are widely applied in studies devoted to the location of faults and to monitor seismic activities. Up to now, its migration mechanism in soil is not fully understood. A systematic soil gas survey across an active fault in NW Taiwan provides the opportunity to closely examine the mechanism of He migration in the fault zone. Significant spatial and temporal correlations observed between soil N_2 and He gas support the hypothesis that N_2 is the probable carrier gas for He emission in the studied area. Based on N_2/Ar ratios and N_2 isotopic results, the excess soil N_2 in this study is considered to be largely derived from ancient atmospheric air which was dissolved in groundwater. Furthermore, observations rule out the possibility of CO_2 being the dominant carrier gas for He in the studied area based on the C and He isotopic compositions and the relationship between concentrations of these gases. At least two soil gas sources, A and B, can be identified in the studied area. Source A is an abiogenic gas source characterized by excess N_2 and He, and very low O_2 and CO_2 content. Source B, on the other hand, is a mixture of biogenic gas and atmospheric air. The development of the fault system is an important factor affecting the degree of mixture between sources A and B. Therefore, variations of soil gas composition, in particular those derived from source A, could be a useful proxy for tracing faults in the area.

1. Introduction

Trace gas is one of the most useful tools which have been applied to discover and delineate faults (e.g. Ciotoli et al., 1998; Toutain and Baubron, 1999; Fu et al., 2005, 2008; Walia et al., 2005b, 2008), study/monitor seismic activities (e.g. Tsunogai and Wakita, 1995; Sano et al., 1998; Italiano et al., 2001; Gulec et al., 2002; Chyi et al., 2005; Walia et al., 2005c; Yang et al., 2005b, 2006b; Fu et al., 2009), study/monitor volcanic activities (e.g. Sano and Wakita, 1985; Hilton et al., 2000, 2002; Lee et al., 2008) and as an indicator for fluid sources (e.g. Tedesco and Scarsi, 1999; Van Soest et al., 2002; Jaffe et al., 2004; Chen et al., 2005; Walia et al., 2005a; Yang et al., 2003a, 2004, 2005a). Helium-4 (hereafter simply referred to as He) is important for these purposes, because of its unique characteristics of being chemically inert, of non-biogenic origin, and being highly mobile, relatively insoluble in water, and radioactively stable (Reimer, 1980; Ozima and Podosek, 2002; Yang et al., 2009). Despite its importance, its migration mechanism is still debated.

In this study, a soil gas survey across the Hsincheng Fault (Fig. 1a and b), which is an active fault in NW Taiwan, was conducted. Various gas concentrations (He, Ar, O_2, CO_2, N_2) and isotopic compositions ($^3He/^4He$, $\delta^{13}C_{CO2}$ and $\delta^{15}N_{N2}$) were determined in order to understand the origin of the soil gases. Weekly monitoring of soil gas concentrations was likewise conducted at a selection of the stations in order to understand the temporal variation of these gas species. The goal of this work is to contribute some observations pertaining to the mechanism of He gas transport. The carrier gas mechanism was considered in this case for He transport (Kristiansson and Malmqvist, 1982). The most likely carrier gas for He, either CO_2 or N_2, which are the dominant soil gases in the study area, will be identified. Methane will not be considered here because it occurs only as a minor component in only three samples. To identify the possible carrier gas of He, the following aspects were studied: (1) the spatial variation of different gas species across the fault zone; (2) the temporal variation of various gases; (3) the origin of the different gases.

2. Principle and methodology

2.1. Principle

Helium has two naturally-occurring radiogenic isotopes: ^3He and ^4He. Most of the ^4He is of radiogenic origin, i.e., the product of alpha decay of radioactive isotopes such as ^{238}U, ^{235}U and

* Corresponding author. Tel./fax: +886 2 2363 6095.
E-mail address: tyyang@ntu.edu.tw (T.F. Yang).

0883-2927/$ - see front matter © 2010 Elsevier Ltd. All rights reserved.
doi:10.1016/j.apgeochem.2010.01.016

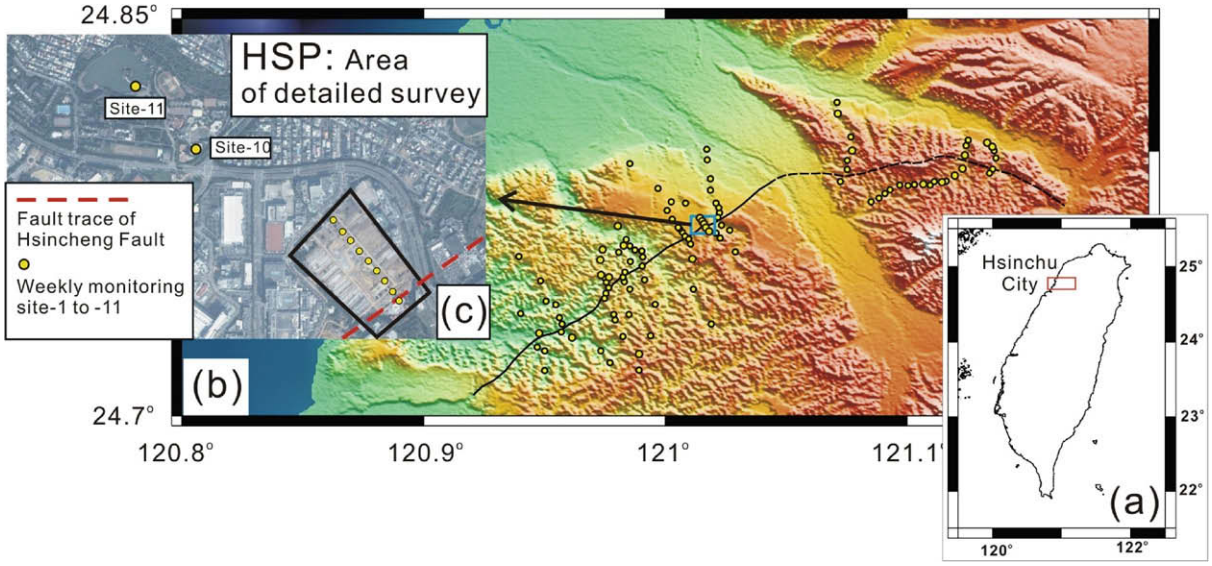

Fig. 1. (a) Location of Hsinchu County in Taiwan. (b) The enlarged map of the rectangle in (a) showing the general survey area and sampling points. The solid line indicates the fault trace of the Hsincheng Fault while the dashed line indicates the suspected extension of the Hsincheng Fault. (c) The enlarged map of the rectangle in (b) showing Hsinchu Science Park (HSP) (background image was modified from Google Earth) and the monitoring sites inside (dots inside rectangle showing site-1 to -9; dots outside the rectangle showing sites -10 and -11). Fault trace is shown by the thick-dashed line.

^{232}Th in the crust. Most of ^{3}He is of primordial origin (Butt et al., 2000; Ozima and Podosek, 2002). Radon (^{222}Rn), which is often used in fault-finding studies (e.g. Fu et al., 2005; Yang, 2008), is produced in the radioactive decay series of ^{238}U. The low diffusion coefficient of He and the short half-life of Rn (3.82 days) do not allow them to migrate to the surface only by diffusion. As a result, the mechanism by which such trace gases (i.e. He and Rn) migrate in the subsurface is still not clear.

Several different mechanisms have been proposed to explain the behavior of trace gas transport. Diffusion has long been considered as an important process for earth degassing (Newton and Round, 1961). However, many problems arise if long-distance transport is considered due to the small diffusion coefficients of trace gases. Helium, for example, has a diffusion coefficient in limestone or saturated rocks in the range from 10^{-4} to 10^{-9} cm^2/s (Pandey et al., 1974; Lerman, 1979). It could only move a few tens of meters through solid rocks even at geological time scales if diffusion were the only mechanism (Etheridge et al., 1984; Gold and Soter, 1984). The other possible mechanisms are advection and groundwater transport. Advection refers to movement of materials under external forces such as pressure gradients. Such a mechanism requires a stream of free gas (a gas domain) which occurs only at sufficiently high concentration (Etiope and Martinelli, 2002). However, trace gases like He usually do not occur in sufficiently high amounts to form a free gas phase. Moreover, such advection/convention flow is usually related to seismic or volcanic activities (King, 1978; Cox, 1980) and hence may not be applicable to the general situation. Newton and Round (1961) suggested that a significant portion of He is dissolved in water so that the migration of He is dominated by water flow. Such a model was supported by some subsequent studies (Eremeev et al., 1973). However, a groundwater transport model can only explain the long-distance transport of Rn under favorable conditions (Mogro-Campero and Fleischer, 1977).

Kristiansson and Malmqvist (1982) first proposed the carrier gas mechanism to explain the transport of Rn. The authors conducted measurements at a Pb mine field and then compared the results with theoretical calculations of the transport rate. Their results revealed that diffusion alone could not explain the long-distance Rn transport; in other words, an ascending stream of gas is required to explain the migration of Rn. However, Rn concentration is never high enough for it to form a gas stream by itself, so that a carrier gas is required. The authors termed this process the carrier gas transport mechanism. It infers that a stream of a carrier gas, forms bubbles in the water-filled cracks or fissures (two domains, water and gas domains co-exist) and carries Rn. The carrier gas moves upward with a velocity much higher than the diffusion rate. This hypothesis was confirmed by additional laboratory experiments and field work (Etiope and Lombardi, 1995, 1996; Yang et al., 2003b; Ciotoli et al., 2005). The carrier gas mechanism was established and largely applied in the study of Rn; CO_2 was considered as the most probable carrier gas for soil Rn (Etiope and Lombardi, 1995; Guerra and Lombardi, 2001; Baubron et al., 2002; Ciotoli et al., 2004).

Although it is well accepted that CO_2 might be the carrier gas for Rn, the mechanism for He migration in the solid earth is still a problem. The possibility of diffusional transport of He within the crust had been ruled out by previous studies (Torgersen and Clarke, 1985; Torgersen, 1989). The possibility of advective transport is also small due to the fact that the He flux is variable and episodic (Torgersen and Clarke, 1992). Moreover, the distinct decoupled nature between the He and Ar flux is difficult to explain by advection (Torgersen et al., 1989). Torgersen (1980) provided a detailed model explaining how He could enter from the solid phase into the liquid phase. In his model, the liquid phase could help He to be transported to the atmosphere. The question then would be which fluid, groundwater or geogas, is the carrier to help He migrate. In this study, field observations are provided to suggest the possible mechanism of He migration in the studied area. Although N_2 is thought to be the most probable carrier gas for He, which could serve as supporting evidence for the carrier gas mechanism, the possibility of a groundwater transport mechanism is not totally dismissed.

2.2. Methodology

A 1.5 m long hollow stainless steel tube, 3 cm in diameter, was used for sampling soil gas. A metal tip was added at the front of the tube in order to penetrate the ground easily. About 1.2 m of the tube was hammered into ground. A thinner but longer pipe was

Table 1
Statistics of gas composition for all the collected samples.

	Mean	Standard deviation	Min	Max	Sampling points
General survey along Hsincheng Fault					
CO_2	2.9%	2.8	0%	13.8%	118
He	5.28 ppm	0.13	5.15 ppm	6 ppm	118
N_2	76.5%	3.4	74.1%	91.2%	118
Detailed survey inside Hsinchu Science Park (HSP)					
CO_2	4.6%	4.1	0%	17.2%	85
He	5.32 ppm	0.15	5.15 ppm	6.07 ppm	85
N_2	79.1%	6.0	73.7%	97.5%	85

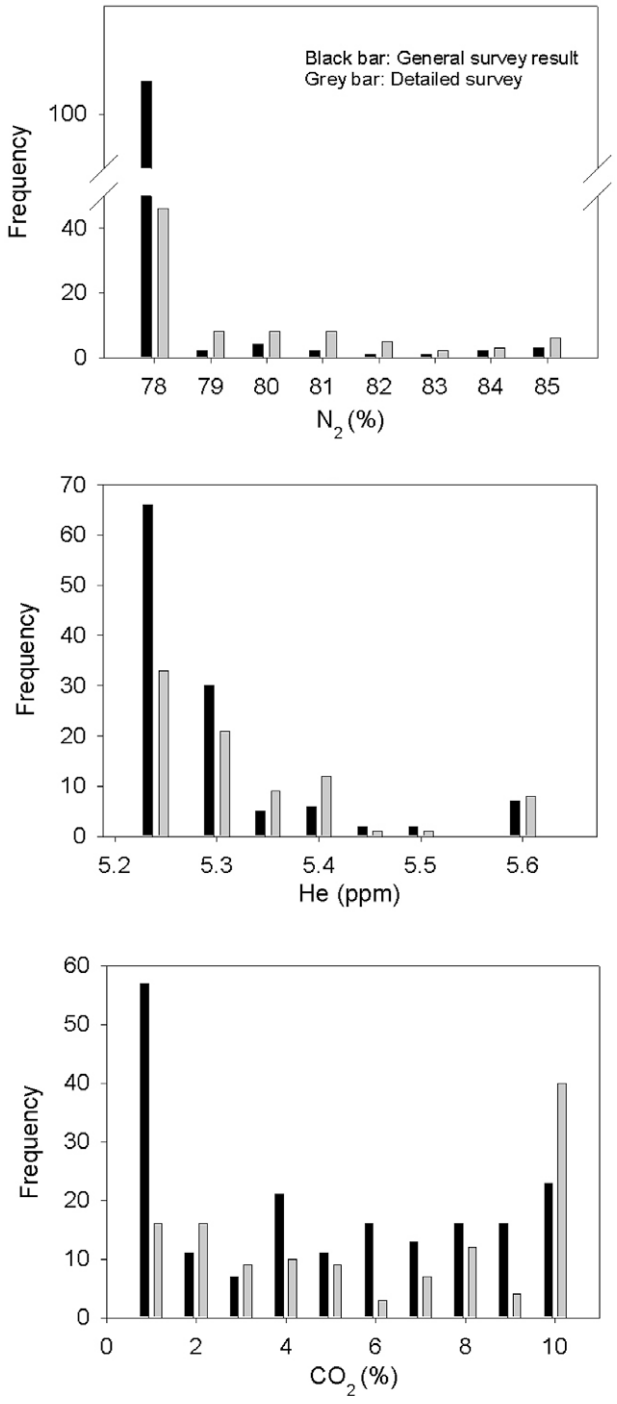

Fig. 2. Distribution of N_2, He and CO_2 concentrations in samples collected during general and detailed surveys. The *x*-axis shows the concentration for each gas species; the *y*-axis shows the number of sample in each concentration range.

Table 2
Gas compositions of samples for carbon, nitrogen and helium isotopic analysis.

Sample no.	Ar (%)	N_2 (%)	O_2 (%)	CO_2 (%)	[^{4}He] (ppm)	N_2/Ar	Excess[b] N_2 (%)
21-1	0.93	87.07	5.62	6.38	5.40	93.3	9.0
21-2	1.03	90.00	3.05	5.92	5.46	85.1[a]	4.0
21-3	1.08	93.74	5.18	n.d.	5.68	87.2	3.8
21-4	1.57	85.14	13.29	n.d.	5.37	54.1	−46
21-5	1.39	85.10	9.79	3.73	5.33	61.2	−31
21-6	0.96	83.45	12.38	3.22	5.33	87.4	3.6
21-7	1.01	85.03	12.00	1.96	5.33	84.2	0.6
21-8	0.99	81.84	17.17	n.d.	5.32	83.1	−0.5
21-9	0.98	82.76	9.21	7.06	5.30	84.8	1.2
21-10	0.95	79.36	18.82	0.88	5.24	83.9	0.3
21-11	0.98	79.41	17.12	2.49	5.24	80.7	−2.8
21-12	1.02	82.91	12.95	3.13	5.28	81.6	−2.1
21-13	0.98	81.01	14.22	3.78	5.24	82.3	−1.3
21-14	0.92	79.57	19.51	n.d.	5.32	86.5	2.7
21-15	1.03	87.20	8.72	3.05	5.40	84.6	1.0
23-1	0.97	81.52	13.14	4.38	5.48	84.4	0.8
23-2	0.98	82.63	12.41	3.98	5.24	84.3	0.7
23-3	1.02	88.93	8.34	1.71	5.08	87.1	3.6
23-4	1.06	89.61	8.16	1.17	n.d.	84.8	1.3
23-5	0.98	88.12	5.92	4.97	5.40	89.6	5.9
23-6	1.01	83.44	10.86	4.70	5.79	82.7	−0.9

n.d.: not detectable.
[a] N_2/Ar ratio of this sample was determined at the Ocean Research Institute of the University of Tokyo.
[b] Excess N_2 is defined as $[N_2]_{sample} - [Ar]_{sample} * (78.082/0.934)$.

then inserted into the hollow tube in order to separate the tip from the hollow tube. The hollow tube was connected to an already designed pipe line and a hand pump or automatic pump; after flushing, the soil gas could be pumped out and stored in vacuum sampling bags or bottles for further analyses.

Soil gas surveys along 11 profiles transecting the Hsincheng Fault, one of the active faults in NW Taiwan, were conducted (Fig. 1a and b). During the 4-month survey, a total number of 118 samples were collected. In addition, 85 samples were collected in a very confined area in the Hsinchu Science Park (HSP) (rectangle in Fig. 1c) in order to determine suitable places for setting up monitoring stations. The distance interval of sampling points is several hundreds to several tens of meters depending on local conditions and the resolution required. For weekly monitoring, 11 temporary monitoring sites (site-1 to -11) were set up along a profile across the Hsincheng Fault inside or near the HSP (Fig. 1c). This profile is about 1.5 km long, and the average distance between each sampling point from site-1 to -9 is ca. 50 m. Sites -10 and -11 were set up as background control points, so they were outside the HSP and away from the fault trace. Site-1 was very close to a trench which was drilled for a paleoseismologic study of the Hsincheng Fault (Chen et al., 2003). Soil gas samples were collected every week from each station for 2 months inside the HSP in order to continuously monitor the concentration variation of several gas species (He, CO_2, N_2, Ar + O_2). Gas compositions of these samples

Table 3
Carbon, nitrogen, and helium isotopic results.

Sample no.	Δ^4He (%)	Ra	[^{4}He/^{20}Ne]	δ^{13}C (‰)	δ^{15}N (‰)	F[a]
21-1	11.6	1.03 ± 0.03	0.33			
21-2	−0.8	1.01 ± 0.06	0.30	−21.87	−0.30 ± 0.01	73
21-3	11.9	0.96 ± 0.03	0.19			
21-4	−1.1	1.05 ± 0.06	0.28			
21-5	17.4	1.01 ± 0.03	0.34	−22.59		75
21-6	14.2	1.00 ± 0.04	0.38	−23.13		77
21-7	1.1	1.04 ± 0.06	0.30	−22.69		76
21-8	−0.7	1.02 ± 0.06	0.32			
21-9	1.5	0.95 ± 0.04	0.35	−22.39		75
21-10	3.4	0.98 ± 0.04	0.32	−14.56		44
21-11	−7.9	1.06 ± 0.06	0.31			
21-12	12.6	1.05 ± 0.04	0.29	−24.18		81
21-13	−1.6	1.01 ± 0.05	0.31	−23.58		79
21-14	4.7	1.04 ± 0.05	0.33	−23.96		81
21-15	7.0	1.07 ± 0.05	0.33	−22.31		74
23-1	4.6	0.97 ± 0.06	0.32	−18.92		61
23-2	0.0	0.96 ± 0.05	0.33	−16.72		53
23-3	−3.1	0.94 ± 0.05	0.31	−21.71		72
23-4	49.3	1.04 ± 0.06	0.29	−18.43		59
23-5	3.1	0.96 ± 0.04	0.31	−25.87		88
23-6	10.4	1.04 ± 0.04	0.34	−24.87		84

[a] F denotes the fraction of mixing between CO_2 from limestone and biogenic processes. End member isotopic value was set to be 0‰ for CO_2 from carbonate and −30‰ which is the mid-point in the range for a biogenic source in Hoefs (2004). F is calculated following: $F * (-30‰) + (1 - F) * (0‰) = \delta^{13}C_{samp}$.

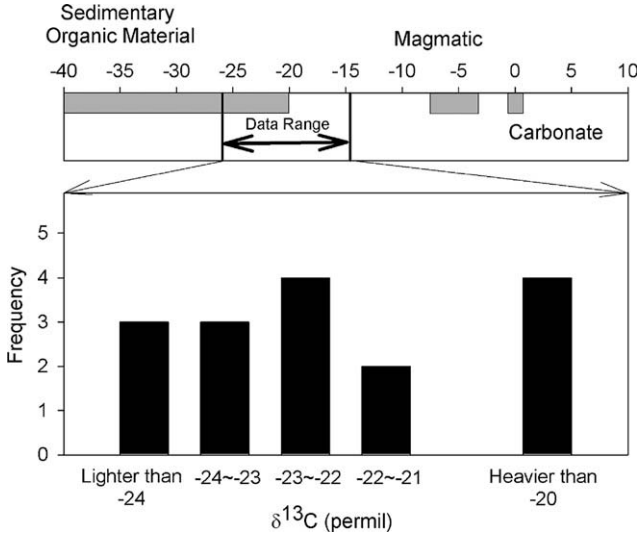

Fig. 3. δ^{13}C values of the soil CO_2 in this study. Grey bars show the ranges for the major components of terrestrial CO_2 sources, based on Hoefs (2004). For CO_2 from carbonate, the δ^{13}C is ~0‰. For a magmatic source, the range is ca. −3.4‰ to −7.8‰. For sedimentary organic material, the range is −20‰ to −40‰. The results show that most soil CO_2 is from sedimentary organic material with little input from carbonate derived CO_2 (gas from a magmatic source is excluded by the He isotopic results; details discussed in text).

were analyzed immediately after collection, by micro gas chromatography (VARIAN CP4900) (for Ar + O_2, N_2 and CO_2; the peaks for O_2 and Ar overlapped each other, so their individual concentration could not be differentiated), and He leak detector (ASM100HDS, Alcatel). Details of analytical procedures and errors were described in Fu et al. (2005) and Walia et al. (2010).

In order to determine He and C isotopes, an additional 21 samples were collected inside the HSP. The gas compositions of these samples were determined by another gas chromatograph (GC, SRI 8610C) with two thermal conductivity detectors (TCD) and one flame ionic detector (FID) in order to differentiate Ar and O_2. For

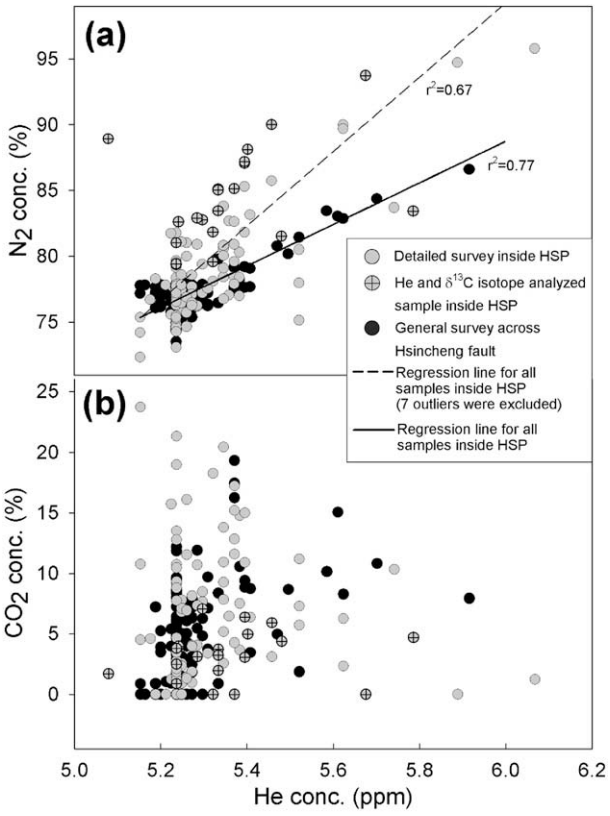

Fig. 4. Correlation between N_2, He and CO_2 concentration. Grey dots are samples collected during the detailed survey; black dots are samples collected during the general survey. All symbols with a cross inside indicate samples with He and δ^{13}C isotopic analysis. (a) Good correlation can be observed between He and N_2. Two proportional correlations were observed indicating that such relationships may vary due to different spatial scales. (b) No significant correlation was observed between He and CO_2 concentrations.

a more detailed description of the analytical procedure has been described by Lee et al. (2005). A noble gas mass spectrometer (Micromass 5400) was used for the analysis of He isotopic ratios and Ne/He ratios. The total error is less than 2.5% including analytical error for samples and working standards and also long-term variations of standards (Yang et al. 2005a, 2006a). Since the soil gas samples are largely affected by atmospheric air, the traditional expression of He isotopic ratio (^{3}He/^{4}He) cannot clearly show the variability in order to determine the origin of the samples. Therefore, results are expressed as the concentration of excess ^{4}He (Δ^4He) which is normalized to atmospheric air concentration. Excess ^{4}He can be expressed as

$$\Delta^4\mathrm{He}(\%) = ([^4\mathrm{He}]_{\text{in sample}} - [^4\mathrm{He}]_{\text{in air}})/[^4\mathrm{He}]_{\text{in air}} \times 100 \quad (1)$$

For $\delta^{13}C_{CO2}$ analysis, CO_2 from soil gas samples was trapped by liquid N_2 in a vacuum gas purification system. Then, the purified CO_2 was sealed in a glass bead for further isotopic analyses using a Finnigan MAT mass spectrometer. One of the samples was sent to the Ocean Research Institute of the University of Tokyo for $\delta^{15}N_{N2}$ and N_2/Ar ratio analysis. Analytical errors for $\delta^{15}N_{N2}$ and N_2/Ar were about 0.3‰ and 3‰, respectively (Takahata et al., 1998). Carbon and N isotopic ratios are expressed relative to Pee Dee Belemnite for C and atmospheric air for N. In order to calculate the excess N_2 concentration relative to atmospheric air, Ar concentration was used as a reference for calculation because Ar concentration is relatively constant compared to O_2 and N_2. In addition, Ar is less affected by the processes discussed here. The calculation is done according to the formula below:

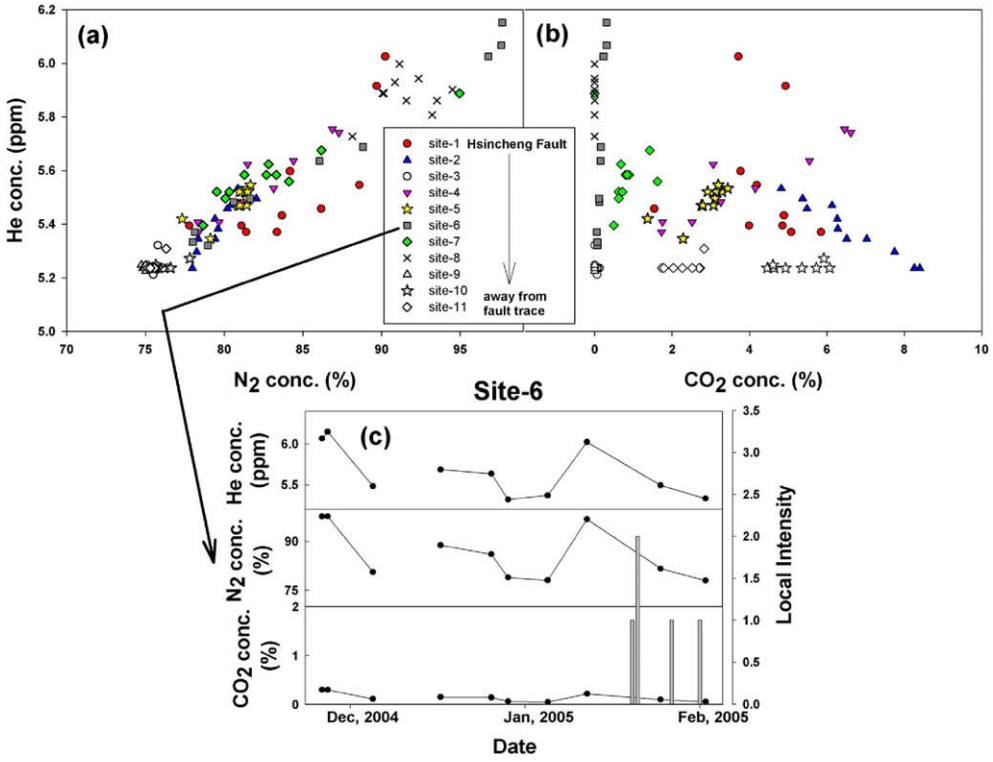

Fig. 5. Weekly monitoring results of 11 monitoring sites. Each symbol indicates an individual site. Points of a symbol refer to samples collected at different dates. (a) Good spatial and temporal correlation could be observed between N_2 and He in most sites (sites -1, -2, -4, -5, -6, -7, -8); poor correlation occurred at sites that are far away from the fault trace (sites -9, -10, -11). This may suggest that distance from the fault trace may also control gas emission. (b) A significant proportional relationship between CO_2 and He occurred only at sites -4 and -5. Most sites do not exhibit significant correlations (or even inverse correlation at site-2). (c) The variation of He, N_2, CO_2 concentration, and local seismic intensity with time in site-6 is plotted as an example showing the temporal variation of different gases and relationship with seismic events.

$$[N_2\text{conc.}]_{\text{excess}} = [N_2\ \text{conc.}]_{\text{sample}} - [\text{Ar conc.}]_{\text{sample}} \times 78.082/0.934 \quad (2)$$

where 78.082 and 0.934 are the percentages of N_2 and Ar for theoretical atmospheric air.

3. Results and discussion

The soil gas survey conducted in this study can be divided into two parts. One is the general survey involving 118 samples, taken along 11 profiles across the Hsincheng Fault; the other is the detailed survey which was focused in the HSP for the purpose of establishing monitoring stations. For the detailed survey, a total of 85 samples were collected within several hundred m^2 inside the HSP. All of these 203 samples were analyzed for N_2, CO_2, Ar + O_2, and He concentration; CH_4 was only found in three samples, so its concentration variation will not be discussed. The means as well as minimum and maximum compositional values are given in Table 1 and Fig. 2. In addition to those 203 samples, another 21 samples were collected for He, $\delta^{13}C_{CO2}$ and $\delta^{15}N_{N2}$ isotopic analysis (Tables 2 and 3). The excess ^{4}He ranges from −7.9 to 49.3. Values of $\delta^{13}C_{CO2}$ fall in the range of −25.9‰ to −14.6‰. These $\delta^{13}C_{CO2}$ values show that CO_2 gas in the study area is dominated by biogenic CO_2 with a small admixture of CO_2 from carbonate (Fig. 3). The $\delta^{15}N_{N2}$ value and N_2/Ar ratio of sample #21-2 are −0.3‰ and 85.1 (Tables 2 and 3), respectively, indicating that the source of N_2 gas is dominated by atmospheric air (Littke et al., 1995). The N_2/Ar ratios of other samples fall within the range of 54.1–93.3 (Table 2) which also indicate the atmospheric-origin of N_2 in the soil gas of this region.

Several lines of evidence, which will be discussed in the following paragraphs, suggest that N_2 is the most probable carrier gas for He emission in the studied area. First, good spatial and temporal correlations are observed for N_2 and He, but do not exist for CO_2 and He. Second, from isotope and gas composition data, CO_2 in the studied area behaves differently from He, suggesting that they are not derived from the same source. A two-source mixing model is proposed to explain the soil gas system and its relationship to the fault system in this area.

Soil N_2 concentrations show a relatively good correlation with He concentration ($r^2 = 0.67$ for the detailed survey and $r^2 = 0.77$ for the general survey), while such a relationship is not observed between CO_2 and He ($r^2 = 0.11$) (Fig. 4a and b), in this study. In Fig. 4a, two proportional relationships could be observed. One is pertaining to the general survey along the 11 profiles across the Hsincheng Fault (black points in Fig. 4a); the other is derived from the detailed survey in the HSP (grey points in Fig. 4a). Two different proportional relationships confirm that such relationship does exist in general but varies due to different sampling locations or resolution. However, such relationships cannot be observed between He and CO_2 (Fig. 4b).

The spatial and temporal relationship between N_2, CO_2 and He is shown in Fig. 5. In Fig. 5a and b, each symbol represents a monitoring station; points with different symbols represent samples collected on different days at that station. The temporal variations are illustrated for site-6 in Fig. 5c as an example. In Fig. 5a, 6 out of 11 stations show good proportional correlation between N_2 and He concentration indicating that their concentrations have the same temporal variation at more than half of the stations. Moreover, the distance away from the fault trace might be one the factors controlling the soil gas He concentrations (and N_2) in the studied area. Systematic variation of the He concentration can be observed from site-1 to -7 (excluding site-3 which might be affected by wet soil); however, such variations could not be observed in samples

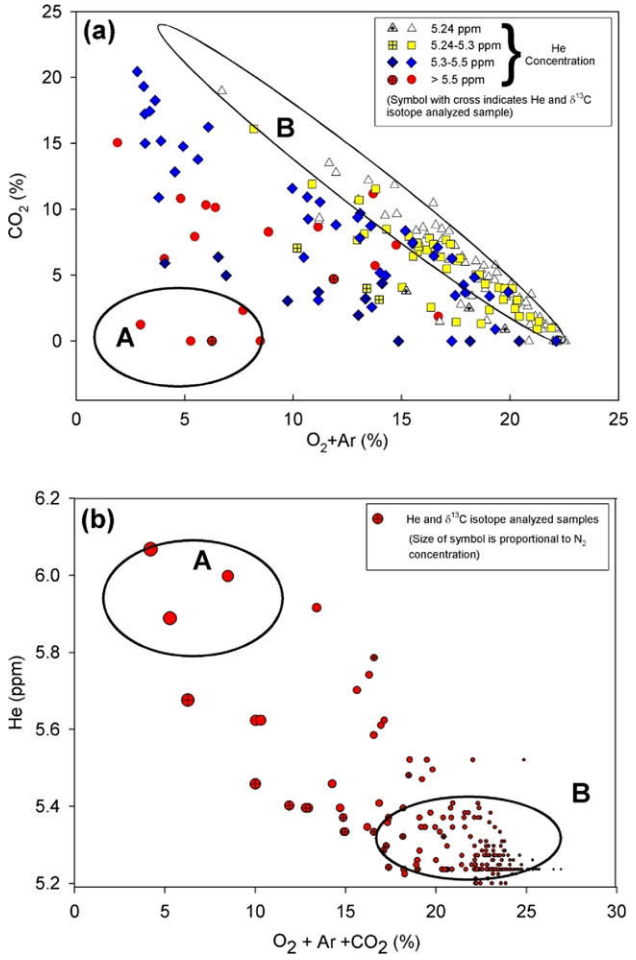

Fig. 6. Scatter plot of the concentrations of various gas species. All symbols with a cross inside indicate samples with He and $\delta^{13}C$ isotopic analysis. (a) All samples can be classified in four categories according to their He concentration. Lower CO_2 and O_2 + Ar concentration would be expected as He concentration increases. (b) The correlation between He concentration and the sum of Ar, O_2 and CO_2 indicating the inverse relationship. The size of the symbols is proportional to the N_2 concentration. Two sources could be identified from the figure. Source A is the source with high He and N_2-content while both CO_2 and O_2 contents are low. Source B is the source with a constant concentration sum of O_2, Ar, and CO_2 while N_2 and He concentrations are close to the atmospheric air value. The CO_2 and O_2 content in source B would follow an inverse proportional relationship indicating variable degrees of atmospheric air content and/or microbial activity involvement.

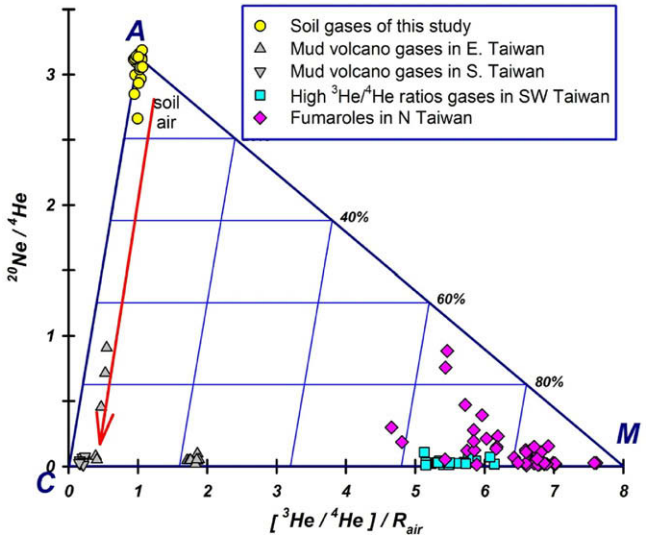

Fig. 7. Three-component plot of He and Ne isotopes for soil gas samples in this study. Gas samples from mud volcanoes in southern Taiwan and fumarole samples from northern Taiwan are also shown for comparison (data sources: Yang et al., 2003a, b; Lan et al., 2007; Lee et al., 2008). A: air; C: crust; M: mantle component.

collected from site-8 to -11. As shown in Fig. 5c, the He and N_2 concentration of site-6, as an example, have very similar temporal variation. On the other hand, such a variation is not clear between CO_2 and He at this site. Local intensity of seismic events during that time period is also shown in the figure indicating that some relationship between seismic activities and He and N_2 concentration may exist. However, the temporal resolution of the sampling is insufficient to identify the relationship at this stage. A long term continuous monitoring station has been set up in order to verify the real cause of the gas variations (Walia et al., 2009).

In Fig. 5b, a poor correlation is observed between CO_2 and He concentrations. Some sites do show a proportional correlation, for examples, sites -4 and -5. However, other sites exhibit inverse proportional relationships (site-2) or no significant relationship (sites -1, -3, -6, -7, -8, -9, -10 and -11). In particular, very different behavior between CO_2 and He was observed for some sites. High CO_2 but low He concentrations were observed at sites -9 and -10; whereas low CO_2 but high He concentrations were observed at sites -6 and -8, suggesting that degassing of CO_2 and He are related to different mechanisms. In summary thus, the above discussions show that good spatial and temporal relationships exist between N_2 and He but not between CO_2 and He. Such relationships indicate that N_2 is the most plausible carrier gas for He in this area.

The relationship between CO_2, Ar + O_2, and He concentration is shown in Fig. 6a. If only samples with a He concentration equal to 5.24 ppm (triangles in Fig. 6a) are considered, their CO_2 and Ar + O_2 concentration show an inverse proportional relationship. This might represent the differing contents of air. Another explanation is that O_2 derived from air was consumed by biogenic processes producing CO_2 (Rixon and Bridge, 1968; Ross and Roberts, 1970; Gregory and Durrance, 1985; Lovell, 2000); thus, this relationship may represent the involvement of biogenic processes. No matter which process occurred in the studied area, they both indicate that the gas is derived from shallow sources.

If the samples with He concentration >5.24 ppm are further considered, a progressive trend could be observed in that He concentration increases as both CO_2 and O_2 concentrations decrease (Fig. 6a). This trend is further demonstrated in Fig. 6b where He concentration was plotted versus the sum of CO_2 and O_2 concentrations. As CO_2 and O_2 concentration decrease, both N_2 and He concentration increase, but it must be noted that if a gas is removed from a gas mixture, the concentration of remaining components increases. The increase of N_2 concentration could probably be a consequence of decreasing CO_2 and O_2 concentration. However, in samples with high He concentration, N_2 is the only gas left implying that N_2 is the only possible carrier for He. The amount of excess N_2 may be calculated on the basis of the Ar content in the soil gas samples if it is assumed all of the Ar is from air. As shown in Table 2, up to 9% of excess N_2 was obtained indicating that not all of the N_2 in the soil gas is from modern air. Another source with high N_2 concentration is required to explain the excess gas. So far, it has been shown that the degassing behavior of He and CO_2 is very different, so that it is difficult to argue for CO_2 as a unique phase to carry He. Moreover, a source with high N_2 concentration is required. Such a high N_2-content source might also to be characterized by high He-content based on the proportional relationship between N_2 and He (Fig. 4a).

The observation that He and CO_2 might be derived from different sources could be further verified by their isotopic

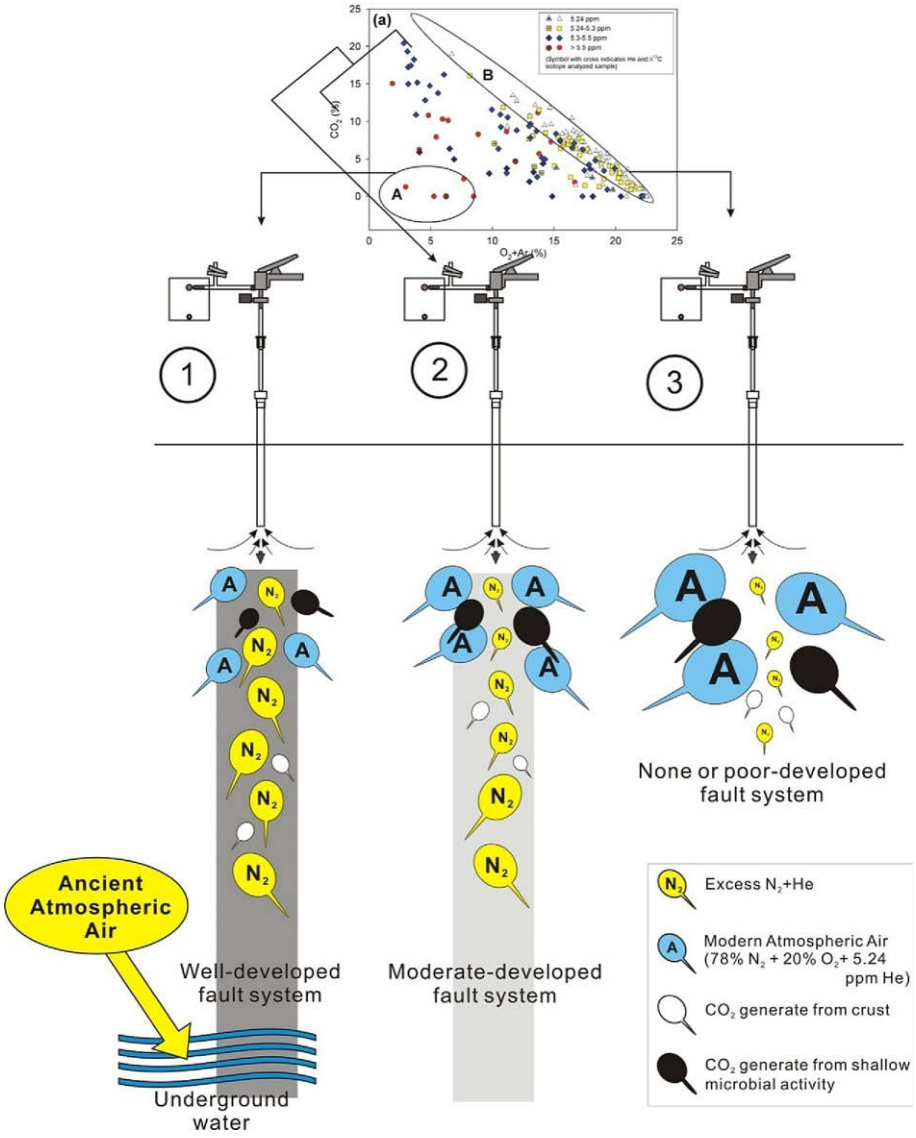

Fig. 8. Sketch of the model explaining the gas mixtures and migration mechanisms in the study area. Three groups of gas behaviors were distinguished. (1) A well-developed fault system serves as a pathway for excess N_2 and He for migrating upward. The excess N_2 observed might be derived from ancient atmospheric air dissolved in groundwater. Very little admixture from source B is observed. (2) Where only a moderately-developed fault system exists, less excess N_2 and He migrate upward. Some degree of admixture from source B is observed. (3) In poorly-developed fault systems soil gas is dominated by atmospheric or biogenic gas.

compositions. Based on the He isotopic results (Fig. 7), the soil gases are dominated by an air component with some crustal input. Gas from a magmatic source could be ruled out; otherwise, some signal should be observed in the He isotopic data. Based on the $\delta^{13}C_{CO2}$ value ($-25.9 \sim -14.6‰$), CO_2 is considered to be dominated by a biogenic source (~70–80%), which is impossible for He generation. Regarding the source of excess N_2 in the studied area, the $\delta^{15}N_{N2}$ value ($-0.3‰$) and N_2/Ar ratio (85.1) (Table 3), both indicate an atmospheric air source of N_2. This implies that the excess N_2 might be derived from ancient atmospheric air which dissolved in groundwater. During the residence in the aquifer, most O_2 in ancient atmospheric air was consumed due to its higher activity. As a result, while the groundwater is flowing across a fault zone, excess N_2 carrying He can be released from the groundwater and enter into surrounding soil gas. This could also indicate that the carrier gas mechanism is capable of explaining the transport of He in the studied area.

A model is proposed to explain the soil gas system in the studied area. Two sources of soil gases in this region could be defined from Fig. 6a and b. Source A is characterized by (1) excess He and N_2, (2) none or very low CO_2, O_2 and Ar contents; (3) CO_2 and O_2 concentration do not follow the inverse proportional relationship observed in source B. The characteristics of source B are: (1) He and N_2 concentrations are close to atmospheric air values; (2) CO_2 and Ar + O_2 concentration follows an inverse proportional relationship. From these characteristics and the isotopic characteristics, it is believed that source B is a mixture of atmospheric air and biogenic gas, whereas source A is considered as abiogenic gas ultimately derived from ancient atmospheric air that dissolved in underground water. During the transport of groundwater, most O_2 was consumed by some microbial activities or reactions with host rocks. The dissolved ancient air contributes the excess N_2 in source A. Where the fault system is well-developed, the gas from source A might carry He and migrate upward.

Considering the two-source model and that distance from the fault trace may affect gas behavior, the gas samples were classified into three groups (Fig. 8). Group 1 is where gas from source A migrates rapidly through a well-developed fault system; during the

migration there is none or very little influence from other sources. Group 1 could correspond to those samples with He concentration >5.5 ppm (squares in Fig. 6a). Group 2 represents gas samples that are mixtures of sources A and B which could correspond to samples with He concentrations >5.5 ppm but <5.24 ppm (diamonds and squares in Fig. 6a). Samples in this group represent gas migrating through an only moderately-developed fault system, so that it suffers a certain degree of mixture with source B. Group 3, which could correlate to samples with He concentrations equal to 5.24 ppm (triangles in Fig. 6a), represents the condition where no or only a poorly-developed fault system exist. Because there is no pathway for gas from source A to migrate, He and N_2 concentration is close to the value of atmospheric air.

4. Conclusions

(1) Significant correlations are observed in this study between soil gas concentrations of N_2 and He. Such a relationship is not observed between CO_2 and He.
(2) The monitoring results show that the distance from the fault trace might be one factor controlling the variations of the He concentration suggesting that the fault system could provides pathways for gas to migrate upward from deep sources.
(3) The isotopic composition of the gases enables identification of the origins of soil CO_2, He and N_2: CO_2 is dominated by biogenic sources with little input from carbonate sources, and He is dominated by atmospheric gas with some input from the crust; N_2 is dominantly derived from ancient atmospheric air.
(4) Nitrogen is enriched by up to 9% relative to air suggesting that not all of the N_2 observed in soil gas is derived from modern atmospheric air; some might be from ancient atmospheric air. Ancient atmospheric air that dissolved in underground water contributes the excess N_2 and is the most probable carrier gas for He in this area.
(5) It is proposed that the carrier gas mechanism is the most plausible mechanism to explain the transport of He in this study and that N_2 is the most probable carrier gas. A two-source mixing model is proposed to explain the soil gas system in this area. Source A is characterized by high He and N_2 and low CO_2 and O_2 contents. In source B, CO_2 and O_2 contents follow an inverse proportional relationship indicating different degrees of air content or involvement of microbial activities. Helium and N_2-contents in source B are close to the value of the atmospheric air.

Acknowledgements

Authors would like to thank K.W. Wu, B.W. Lin, C.C. Wu, T.H. Wang and H.F. Lee at the Department of Geosciences of NTU for helping in the collection and analysis of the samples. T.F. Lan and M. Nishizawa helped with nitrogen isotopic analysis. Dr. G. Martinelli and an anonymous reviewer gave critical comments. Mrs. M. Walia and Dr. U. Knittel improved the manuscript. The National Science Council (NSC93-2815-C-002-035-M), National Center for Research on Earthquake Engineering, and Central Geological Survey of Taiwan financially support this research.

References

Baubron, J.C., Rigo, A., Toutain, J.P., 2002. Soil gas profiles as a tool to characterize active tectonic areas: the Jaut Pass example (Pyrenees, France). Earth Planet. Sci. Lett. 196, 69–81.

Butt, C.R.M., Gole, M.J., Dyck, W., 2000. Helium. In: Hale, M. (Ed.), Geochemical remote sensing of the sub-surface. Elsevier, pp. 303–352. Chapter 10.

Chen, W.S., Liu, L.H., Yan, Y.C., Yang, H.C., Lee, L.S., Yu, N.T., Chang, H.C., Shih, R.C., Chen, Y.G., Lee, Y.H., Lin, W.H., Shih, T.S., Lu, S.T., 2003. Paleoseismologic study of the Hsincheng Fault. Special Publication Central Geological Survey 14, 11–24 (in Chinese with English abstract).

Chen, C.T.A., Zeng, Z.G., Kuo, F.W., Yang, T.F., Wang, B.J., Tu, Y.Y., 2005. Tide-influenced acidic hydrothermal system offshore NE Taiwan. Chem. Geol. 224, 69–81.

Chyi, L.L., Quick, T.J., Yang, T.F., Chen, C.H., 2005. Soil gas radon spectra and earthquakes. Terr. Atmos. Ocean. Sci. 16, 763–774.

Ciotoli, G., Guerra, M., Lombardi, S., Vittori, E., 1998. Soil gas survey for tracing seismogenic faults: a case study in the Fucino basin, central Italy. J. Geophys. Res. 103, 23781–23794.

Ciotoli, G., Lombardi, S., Morandi, S., Zarlenga, F., 2004. A multidisciplinary, statistical approach to study the relationships between helium leakage and neotectonic activity in a gas province. The Vasto basin Abruzzo-Molise (central Italy). Am. Assoc. Petrol. Geol. Bull. 88, 355–372.

Ciotoli, G., Etiope, G., Guerra, M., Lombardi, S., Duddridge, G.A., Grainger, P., 2005. Migration of gas injected into a fault in low-permeability ground. Quart. J. Eng. Geol. Hydrogeol. 38, 305–320.

Cox, M.E., 1980. Ground radon survey of a geothermal area in Hawaii. Geophys. Res. Lett. 7, 283–286.

Eremeev, A.N., Sokolov, V.A., Solovov, A.P., Yanitskii, I.N., 1973. Applications of helium surveying to structural mapping and ore deposit forecasting. In: Jones, M.J. (Ed.), Geochemical Exploration 1972. Institution of Mining and Metallurgy, London, pp. 183–192.

Etheridge, M.A., Wall, V.J., Cox, S.F., Vernon, R.H., 1984. High fluid pressure during regional metamorphism and deformation – implications for mass-transport and deformation mechanisms. J. Geophys. Res. 89, 4344–4358.

Etiope, G., Lombardi, S., 1995. Evidence for radon transport by carrier gas through faulted clays in Italy. J. Radioanal. Nucl. Chem. 193, 291–300.

Etiope, G., Lombardi, S., 1996. Laboratory simulation of geogas microbubble flow. Environ. Geol. 27, 226–232.

Etiope, G., Martinelli, G., 2002. Migration of carrier and trace gases in the geosphere: an overview. Phys. Earth Planet. Interiors 129, 185–204.

Fu, C.C., Yang, T.F., Walia, V., Chen, C.H., 2005. Reconnaissance of soil gas composition over the buried fault and fracture zone in southern Taiwan. Geochem. J. 39, 427–439.

Fu, C.C., Yang, T.F., Du, J., Walia, V., Chen, Y.G., Liu, T.K., Chen, C.H., 2008. Variations of helium and radon concentrations in soil gases from an active fault zone in southern Taiwan. Radiat. Meas. 43, S348–S352.

Fu, C.C., Yang, T.F., Walia, V., Liu, T.K., Lin, S.J., Chen, C.-H., Hou, C.S., 2009. Variations of soil-gas composition around the active Chihshang Fault in a plate suture zone, eastern Taiwan. Radiat. Meas. 44, 940–944.

Gold, T., Soter, S., 1984. Fluid ascent through the solid lithosphere and its relation to earthquakes. Pure Appl. Geophys. 122, 492–530.

Gregory, R.G., Durrance, E.M., 1985. Helium, carbon-dioxide and oxygen soil gases – small-scale variations over fractured ground. J. Geochem. Explor. 24, 29–49.

Guerra, M., Lombardi, S., 2001. Soil–gas method for tracing neotectonic faults in clay basins: the Pisticci field (Southern Italy). Tectonophysics 339, 511–522.

Gulec, N., Hilton, D.R., Mutlu, H., 2002. Helium isotope variations in Turkey: relationship to tectonics, volcanism and recent seismic activities. Chem. Geol. 187, 129–142.

Hilton, D.R., Thirlwall, M.F., Taylor, R.N., Murton, B.J., Nichols, A., 2000. Controls on magmatic degassing along the Reykjanes Ridge with implications for the helium paradox. Earth Planet. Sci. Lett. 183, 43–50.

Hilton, D.R., Fischer, T.P., Marty, B., 2002. Noble gases and volatile recycling at subduction zones. In: Porcelli, D., Ballentine, C.J., Wieler, R. (Eds.), Reviews in Mineralogy and Geochemistry, vol. 47. Mineralogical Society of America, pp. 319–370.

Hoefs, J., 2004. Stable Isotope Geochemistry. Springer, Berlin. pp. 31–76, Chapter 2.

Italiano, F., Martinelli, G., Nuccio, P.M., 2001. Anomalies of mantle-derived helium during the 1997–1998 seismic swarm of Umbria-Marche, Italy. Geophys. Res. Lett. 28, 839–842.

Jaffe, L.A., Hilton, D.R., Fischer, T.P., Hartono, U., 2004. Tracing magma sources in an arc–arc collision zone: helium and carbon isotope and relative abundance systematics of the Sangihe Arc, Indonesia. Geochem. Geophys. Geosys. 5, Q04J10. doi:10.1029/2003GC000660.

King, C.Y., 1978. Radon emanation on San-Andreas Fault. Nature 271, 516–519.

Kristiansson, K., Malmqvist, L., 1982. Evidence for nondiffusive transport of Rn-222 in the ground and a new physical model for the transport. Geophysics 47, 1444–1452.

Lan, T.F., Yang, T.F., Lee, H.F., Chen, Y.G., Chen, C.H., Song, S.R., Tsao, S., 2007. Compositions and flux of soil gas in Liu-Huang-Ku hydrothermal area, northern Taiwan. J. Volc. Geotherm. Res. 165, 32–45.

Lee, H.F., Yang, T.F., Lan, T.F., Song, S.R., Tsao, S., 2005. Fumarolic gas composition of the Tatun Volcano Group, northern Taiwan. Terr. Atmos. Ocean. Sci. 16, 843–864.

Lee, H.F., Yang, T.F., Lan, T.F., Chen, C.H., Song, S.R., Tsao, S., 2008. Temporal variations of gas compositions of fumaroles in the Tatun Volcano Group, northern Taiwan. J. Volc. Geotherm. Res. 178, 624–635.

Lerman, A., 1979. Geochemical Processes. Water and Sediment Environments. Wiley, New York.

Littke, R., Krooss, B., Idiz, E., Frielingsdorf, J., 1995. Molecular nitrogen in natural-gas accumulations – generation from sedimentary organic-matter at high-temperatures. Am. Assoc. Petrol. Geol. Bull. 79, 410–430.

Lovell, J.S., 2000. Oxygen and carbon dioxide in soil air. In: Hale, M. (Ed.), Geochemical Remote Sensing of the Sub-Surface, vol. 7. Elsevier, pp. 451–469. Chapter 14.

Mogro-Campero, A., Fleischer, R.L., 1977. Subterrestrial fluid convection: a hypothesis for long-distance migration of radon within the earth. Earth Planet. Sci. Lett. 34, 321–325.
Newton, R., Round, G.F., 1961. The diffusion of helium through sedimentary rocks. Geochim. Cosmochim. Acta 22, 106–132.
Ozima, M., Podosek, F.A., 2002. Noble Gas Geochemistry. Cambridge University Press, London.
Pandey, G.N., Rasintek, M., Katz, D.L., 1974. Diffusion of fluids through porous media with implication in petroleum geology. Am. Assoc. Petrol. Geol. Bull. 58, 291–303.
Reimer, G.M., 1980. Use of soil–gas He concentrations for earthquake prediction: limitations imposed by diurnal variations. J. Geophys. Res. 85, 3107–3144.
Rixon, A.J., Bridge, B.J., 1968. Respiratory quotient arising from microbial activity in relation to matric suction and air filled pore space of soil. Nature 218, 961–962.
Ross, D.J., Roberts, H.S., 1970. Enzyme activities and oxygen uptakes of soils under pasture in temperature and rainfall sequences. J. Soil Sci. 21, 368–381.
Sano, Y., Wakita, H., 1985. Geographical-distribution of $^{3}He/^{4}He$ ratios in Japan – implications for arc tectonics and incipient magmatism. J. Geophys. Res. 90, 8729–8741.
Sano, Y., Takahata, N., Igarashi, G., Koizumi, N., Sturchio, N.C., 1998. Helium degassing related to the Kobe earthquake. Chem. Geol. 150, 171–179.
Takahata, N., Nishio, Y., Yoshida, N., Sano, Y., 1998. Precise isotopic measurements of nitrogen at the sub-nanomole level. Anal. Sci. 14, 485–491.
Tedesco, D., Scarsi, P., 1999. Chemical (He, H_2, CH_4, Ne, Ar, N_2) and isotopic (He, Ne, Ar, C) variations at the Solfatara crater (southern Italy): mixing of different sources in relation to seismic activity. Earth Planet. Sci. Lett. 171, 465–480.
Torgersen, T., 1980. Controls on pore-fluid concentration of ^{4}He and ^{222}Rn and the calculation of $^{4}He/^{222}Rn$ ages. J. Geochem. Explor. 13, 57–75.
Torgersen, T., 1989. Terrestrial helium degassing fluxes and the atmospheric helium budget – implications with respect to the degassing processes of continental-crust. Chem. Geol. 79, 1–14.
Torgersen, T., Clarke, W.B., 1985. Helium accumulation in groundwater (1). An evaluation of sources and the continental flux of crustal He-4 in the Great Artesian Basin, Australia. Geochim. Cosmochim. Acta 49, 1211–1218.
Torgersen, T., Clarke, W.B., 1992. Geochemical constraints on formation fluid ages, hydrothermal heat-flux, and crustal mass-transport mechanisms at Cajon Pass. J. Geophys. Res. 97, 5031–5038.
Torgersen, T., Kennedy, B.M., Hiyagon, H., Chiou, K.Y., Reynolds, J.H., Clarke, W.B., 1989. Argon accumulation and the crustal degassing flux of Ar-40 in the Great Artesian Basin, Australia. Earth Planet. Sci. Lett. 92, 43–56.
Toutain, J.P., Baubron, J.C., 1999. Gas geochemistry and seismotectonics: a review. Tectonophysics 304, 1–27.
Tsunogai, U., Wakita, H., 1995. Precursory chemical changes in ground water – Kobe Earthquake, Japan. Science 269, 61–63.
Van Soest, M.C., Hilton, D.R., Macpherson, C.G., Mattey, D.P., 2002. Resolving sediment subduction and crustal contamination in the Lesser Antilles island Arc: a combined He–O–Sr isotope approach. J. Petrol. 43, 143–170.
Walia, V., Quattrocchi, F., Virk, H.S., Yang, T.F., Pizzino, L., Bajwa, B.S., 2005a. Radon, helium and uranium survey in some thermal springs located in NW Himalayas, India: mobilization by tectonic features or by geochemical barriers? J. Environ. Monitor. 7, 850–855.
Walia, V., Su, T.C., Fu, C.C., Yang, T.F., 2005b. Spatial variations of radon and helium concentrations in soil–gas across the Shan-Chiao fault, Northern Taiwan. Radiat. Meas. 40, 513–516.
Walia, V., Virk, H.S., Yang, T.F., Mahajan, S., Walia, M., Bajwa, B.S., 2005c. Earthquake prediction studies using radon as a precursor in N-W Himalayas, India: a case study. Terr. Atmos. Ocean. Sci. 16, 775–804.
Walia, V., Mahajan, S., Kumar, A., Singh, S., Bajwa, B.S., Dhar, S., Yang, T.F., 2008. Fault delineation study using soil–gas method in the Dharamsala area, NW Himalayas, India. Radiat. Meas. 43, S337–S342.
Walia, V., Yang, T.F., Hong, W.L., Lin, S.J., Fu, C.C., Wen, K.L., Chen, C.-H., 2009. Geochemical variation of soil–gas composition for fault trace and earthquake precursory studies along the Hsincheng Fault in NW Taiwan. Appl. Radiat. Isotopes 67, 1855–1863.
Walia, V., Lin, S.J., Fu, C.C., Yang, T.F., Wen, K.L., Chen, C.-H., 2010. Soil-gas monitoring: A tool for fault delineation studies along Hsinhua Fault (Tainan), Southern Taiwan. Appl. Geochem. 25 (4), 602–607.
Yang, T.F., 2008. Recent progress in the application of gas geochemistry: examples from Taiwan and the 9th International Gas Geochemistry Conference. Geofluids 8, 219–229.
Yang, T.F., Chen, C.H., Tien, R.L., Song, S.R., Liu, T.K., 2003a. Remnant magmatic activity in the Coastal Range of East Taiwan after arc-continent collision: fission-track data and $^{3}He/^{4}He$ ratio evidence. Radiat. Meas. 36, 343–349.
Yang, T.F., Chou, C.Y., Chen, C.H., Chyi, L.L., Jiang, J.H., 2003b. Exhalation of radon and its carrier gases in SW Taiwan. Radiat. Meas. 36, 425–429.
Yang, T.F., Yeh, G.H., Fu, C.C., Wang, C.C., Lan, T.F., Lee, H.F., Chen, C.H., Walia, V., Sung, Q.C., 2004. Composition and exhalation flux of gases from mud volcanoes in Taiwan. Environ. Geol. 46, 1003–1011.
Yang, T.F., Lan, T.F., Lee, H.F., Fu, C.C., Chuang, P.C., Lo, C.H., Chen, C.H., Chen, C.T.A., Lee, C.S., 2005a. Gas compositions and helium isotopic ratios of fluid samples around Kueishantao, NE offshore Taiwan and its tectonic implications. Geochem. J. 39, 469–480.
Yang, T.F., Walia, V., Chyi, L.L., Fu, C.C., Chen, C.H., Liu, T.K., Song, S.R., Lee, C.Y., Lee, M., 2005b. Variations of soil radon and thoron concentrations in a fault zone and prospective earthquakes in SW Taiwan. Radiat. Meas. 40, 496–502.
Yang, T.F., Chuang, P.C., Lin, S., Chen, J.C., Wang, Y., Chung, S.H., 2006a. Methane venting in gas hydrate potential area offshore of SW Taiwan: evidence of gas analysis of water column samples. Terr. Atmos. Ocean. Sci. 17, 933–950.
Yang, T.F., Fu, C.C., Walia, V., Chen, C.H., Chyi, L.L., Liu, T.K., Song, S.R., Lee, M., Lin, C.W., Lin, C.C., 2006b. Seismo-geochemical variations in SW Taiwan: multi-parameter automatic gas monitoring results. Pure Appl. Geophys. 163, 693–709.
Yang, T.F., Marty, B., Hilton, D.R., Kurz, M.D., 2009. Geochemical applications of noble gases. Chem. Geol. 266, 1–3.